PHARMACEUTICAL BIOLOGY
2022, VOL. 60, NO. 1, 1394–1406
https://doi.org/10.1080/13880209.2022.2103718

Taylor & Francis
Taylor & Francis Group

RESEARCH ARTICLE

OPEN ACCESS Check for updates

Network pharmacology approach to investigate the multitarget mechanisms of Zhishi Rhubarb Soup on acute cerebral infarction

Yuejia Shao[a,b], Yue Zhang[a,b], Rongrong Wu[a,b], Lurui Dou[a,b], Fengjiao Cao[a,b], Yuqing Yan[a,b], Yuming Tang[c], Chi Huang[b], Yang Zhao[b] and Jinghua Zhang[b]

[a]Nanjing University of Traditional Chinese Medicine, Nanjing, People's Republic of China; [b]Nanjing Chinese Medicine Hospital Affiliated to Nanjing University of Traditional Chinese Medicine, Nanjing City, People's Republic of China; [c]Yancheng Binhai Hospital of Traditional Chinese Medicine, Yancheng City, People's Republic of China

ABSTRACT

Context: Zhishi Rhubarb Soup (ZRS) is a traditional Chinese medicine formula used in the clinic to treat acute cerebral infarction (ACI) for many years. However, the exact mechanism of the treatment remains unclear.

Objective: This study elucidates the multitarget mechanisms underlying the effects of ZRS on ACI using network pharmacology analysis and verify its effect by performing animal experiments.

Materials and methods: Using the network pharmacology approach, the multiple components, critical targets and potential mechanisms of ZRS against ACI were investigated. Six herbal names of ZRS and 'acute cerebral infarction' were used as keywords to search the relevant databases. In addition, we established the MCAO model to verify the results of network pharmacology enrichment analysis. ZRS (10 g crude drug/kg) was gavaged once per day for 7 consecutive days beginning 3 h after model establishment. After ZRS treatment, TTC staining, Western blot analysis, IHC and ELISA were conducted to further explore the mechanism of ZRS intervention in ACI.

Results: The network pharmacology approach identified 69 key targets, 10 core genes and 169 signalling pathways involved in the treatment of ACI with ZRS. *In vivo* experiment showed that ZRS treatment significantly reduced cerebral infarction volume (42.76%). It also reduced the expression level of AGE, RAGE and P65; and inhibited the expression of inflammatory MMP-9 and IFN-γ.

Conclusions: This study demonstrated that ZRS improved cerebral ischaemic injury by inhibiting neuroinflammation partly via the AGE-RAGE signalling pathway. It provides a theoretical basis for the clinical application of ZRS in the treatment of ACI.

ARTICLE HISTORY
Received 30 March 2022
Revised 20 June 2022
Accepted 15 July 2022

KEYWORDS
Ischaemic stroke; traditional Chinese medicine formula; signalling pathways; mechanism of action

Introduction

Acute cerebral infarction (ACI), also known as ischaemic stroke, is the most common acute cerebrovascular disease in the world (Ovbiagele and Nguyen-Huynh 2011). A survey found that it has become one of the three major causes of death in humans, and it leads to high mortality and disability rates (Mo et al. 2020). ACI mainly occurs due to arterial thrombosis that leads to the occlusion of blood vessels and hypoxia of the brain, resulting in complex pathophysiological reactions (George and Steinberg 2015). Oxidative stress and neuroinflammation are two key factors in the cascade reaction after ischaemic stroke (Chen et al. 2020; He et al. 2021). Microglia rapidly accumulate and are activated after cerebral ischaemia (Iadecola and Anrather 2011). Subsequently, macrophages, neutrophils and other related immune cells cross the damaged blood–brain barrier (BBB) and release proinflammatory factors that promote inflammatory activity and tissue damage (Jones et al. 2018; Jayaraj et al. 2019). In addition, microglia and related immune cells are associated with the production of NADPH oxidase and inducible nitric oxide synthase (iNOS), which aggravate the progression of oxidative stress (He et al. 2021). An elevated oxidative stress response leads to irreversible cellular damage, localized brain tissue necrosis or softening, and ultimately to neurological impairment (Zhao et al. 2017).

Intravenous thrombolysis and mechanical thrombectomy are currently considered effective treatments for ACI and have been shown to improve blood circulation in ischaemic areas as early as possible but within a strict time window (Lansberg et al. 2009; Rabinstein 2017; Albers et al. 2018; Anderson et al. 2019). Traditional Chinese Medicine has a long history of treating apoplexy (Yang et al. 2021). At present, many prescriptions from the traditional medical system for ischaemic stroke have demonstrated their mechanisms of action through modern pharmacological techniques (Liu et al. 2021; Xu et al. 2022). For example, Buyang Huanwu decoction can promote neurogenesis of hippocampus after ischaemia by reducing cell apoptosis in ischaemic brain tissue (Chen et al. 2020); Sanhua decoction can inhibit the expression of inflammatory factors, reduce neuroinflammation, improve nerve function after stroke, etc. (Zhang et al. 2022). In the acute stage of stroke, most patients are characterized by excess symptoms and deficiency in constitution, usually

CONTACT Jinghua Zhang fsyy00268@njucm.edu.cn Nanjing Chinese Medicine Hospital Affiliated to Nanjing University of Traditional Chinese Medicine, 157 Da Ming Road, Nanjing City, Jiangsu Province 210022, People's Republic of China

accompanied by constipation and other gastrointestinal dysfunction, which leads to an intestinal flora disorder, visceral dysfunction and ultimately aggravation of the disease. Therefore, the treatment of acute ischaemic stroke using the Tiaoqi Tongfu method has achieved a good effect in the clinic (Zhang 2019). ZRS is mainly composed of *Rheum palmatum* (chinese name Da Huang; the root and rhizome of *Rheum palmatum* L. [Polygonaceae]), *Magnoliae officmalis Cortex* (Chinese name Hou Pu; the root and branch bark of *Magnolia officinalis* Rehd.et Wils. [Magnoliaceae]), *Fructus aurantii immaturus* (Chinese name Zhi Shi; the young fruit of *Citrus aurantium* L. [Rutaceae]), *Scutellariae Radix* (Chinese name Huang Qin; comes from the dried root of the medicinal plant *Scutellariae baicalensis* Georgi [Lamiaceae]), *Radix Vladimiriae* (Chinese name Mu Xiang; the dried root of the *Vladimiria souliei* (Franch.) Ling. [Asteraceae]) and *Radix Glycyrrhiza* (Chinese name Gan Cao; the dried root of the *Glycyrrhiza uralensis Fisch*. [Fabaceae]) in a 10:10:10:10:3:3 proportion by weight, which regulate the visceral functional activities of qi and remove phlegm to relax bowels. According to previous studies, ZRS regulates the expression of inflammatory factors in MCAO model rats, inhibit inflammation, promote nerve regeneration and exert protective effects on cerebral ischaemia–reperfusion injury (Zhang, Hui, et al. 2021; Zhang, Shao, et al. 2021). A clinical study found that ZRS can improve the neurological deficits, improve the ability of independent living, alleviate the symptoms of phlegm-heat viscera syndrome (Lv et al. 2022). Recent pharmacological studies have shown that anthraquinone compounds in Da Huang regulate the levels of proinflammatory cytokines such as tumour necrosis factor-α (TNF-α), interleukin-1β (IL-1β) and interleukin-6 (IL-6), thereby inhibiting the occurrence of inflammatory responses (Zhuang et al. 2020). Zhi Shi has also been shown to inhibit inflammation by regulating the MAPK/NF-κB signalling pathway (Zhao 2018). However, the comprehensive ingredients in ZRS and their multiple actions, as well as mechanisms underlying their effects on ACI, have not been further elucidated. The application of compound medicine is a characteristic of TCM treatment, but methods to scientifically explain its mechanism of action remain a difficult problem. The concept of comprehensiveness, systematicness and wholeness of network pharmacology is consistent with the characteristics of multiple compounds, multiple targets and multiple pathways of TCM compounds (Jiao et al. 2021). In this paper, the network pharmacological method was used to construct the herb-component-disease-pathway-target network and then experiments were performed to verify and explore the possible mechanism of action of ZRS in the treatment of ACI.

Materials and methods

Experimental reagents

The primary antibodies for NF-κB p65 (8242) were purchased from Cell Signaling Technology (Danvers, MA); RAGE antibody (ab216329) was purchased from Abcam (Cambridge, MA). The ELISA kits for AGE (H250-1-1), MMP9 (H146-4) and IFN-γ (H025) were purchased from Nanjing Jiancheng Bioengineering Institute (Nanjing, China). All ZRS drugs were purchased from the Department of Pharmacy, Nanjing Chinese Medicine Hospital Affiliated with Nanjing University of Traditional Chinese Medicine (Nanjing, China). They were decocted using a conventional method, condensed to 2.5 g/mL, and stored at 4 °C for future use.

Experimental animals and groups

Male Sprague-Dawley rats weighing 220–250 g were purchased from Shanghai SLAC Laboratory Animal Co., Ltd. (Shanghai, China). The research protocol was approved by the Animal Research Committee of the National Institute of Traditional Chinese Medicine. The ethics commission number is KY2019019. The study was conducted according to the guidelines for the Guide for the Care and Use of Laboratory Animals. All efforts were made to alleviate the suffering of animals and to reduce the number of animals used. According to previous research, the procedure for establishing the MCAO model is based on the thread bolt technique commonly used today (Engel et al. 2011). Specifically, the experimental animals were fixed on the operating table in supine position after inhalation anaesthesia. After the skin was disinfected, and the neck was incised. The common carotid artery and vagus nerve were quickly exposed and separated, and the proximal end of the common carotid artery and the external carotid artery were connected. The internal carotid artery was threaded for use, and a small opening was cut at the upper end of the common carotid artery ligation, extending from the bifurcation of the common carotid artery. Premeasured fishing line was then inserted into the internal carotid artery along the common carotid artery, and the internal carotid artery was ligated when the line reached the specified length (approximately 18–20 mm). Tethers of different diameters were chosen according to the animal's weight and nutrient intake, and then, the incision was sutured. After the operation, the body temperature was maintained at 37 ± 0.5 °C with an irradiation lamp, and the rectal temperature, respiration and heart rate were monitored.

Drug dose selection: In the preliminary animal experimental study, we divided the drug into three dose groups: low dose (5 g crude drug/kg), medium dose (10 g crude drug/kg) and high dose (20 g crude drug/kg). The results showed that the middle dose group and the high dose group could reduce the volume of cerebral infarction in rats, but the large dose rhubarb gastrointestinal excretion caused more damage to the body (Zhang, Hui, et al. 2021). Therefore, in this study, the dose of ZRS was selected to be 10 g crude drug/kg body weight.

All animals were randomly divided into the following three groups using random block design: the control group, the vehicle group and the ZRS group. The control operated rats and MCAO rats were i.g. administered an equal volume of sterile saline once daily after surgery. Rats in the ZRS group were gavaged with ZRS once per day at a dose of 10 g crude drug/kg body weight for 7 consecutive days beginning 3 h after model establishment.

Neurological function assessment

At 2 h after MCAO, neurobehavioural scores were determined in each group using the scoring criteria proposed by Longa: 0 points, normal, without any neurological deficit; one point, mild, the contralateral claw cannot be fully extended; two points, moderate, leaning and rotating in the opposite direction when walking; three points, serious, falling to the opposite side; and four points, no independent walking, consciousness suppression. Animal scoring 0 points, four points, and animals experiencing respiratory distress or premature death, and those found to have subarachnoid haemorrhage at the time of execution were discarded according to the first score, the excluded animals were replaced.

Evaluation of the infarct volume

Neurological function was assessed seven days after the ZRS intervention or non-intervention, and the rats were anaesthetized and sacrificed. The brain was quickly removed, frozen at −20 °C for 15 min, and then cut into coronal sections that were 2 mm thick. The slices were placed in 2% TTC in phosphate-buffered saline (pH 7.4) and incubated at 37 °C in the dark for 30 min. Brain slices were fixed with a 4% paraformaldehyde solution at room temperature. After successful staining, ischaemic brain tissue appeared white. The brain tissue volume was measured using an image processing system (Image-Pro Plus 6.0). The formula is as follows: percentage of infarct volume = (total infarct volume – (ipsilateral hemisphere volume – contralateral hemisphere volume))/contralateral hemisphere volume × 100% (Kong et al. 2014).

Screening of chemical ingredients and targets in ZRS

The chemical ingredients and targets in *Rheum palmatum*, *Magnoliae officmalis Cortex*, *Fructus aurantii immaturus*, *Scutellariae Radix*, *Radix Vladimiriae* and *Radix Glycyrrhiza* were screened from the Traditional Chinese Medicine System Pharmacology Database (TCMSP, https://tcmspw.com/tcmsp.php), which provides comprehensive information about ingredients in herbs (Ru et al. 2014). Oral bioavailability (OB) values greater than or equal to 30% were considered to indicate good absorption after oral administration. A calculated value of drug likeness (DL) no less than 0.18 indicated that the compound had suitable chemical properties for drug development (Zeng et al. 2019). Therefore, the screening conditions for all components were set to an OB $\geq$ 30% and DL $\geq$ 0.18 to identify the possible effective chemical components and targets of the ZRS.

Collection of ACI-related targets

The acknowledged ACI-related targets were collected from GeneCards (https://www.genecards.org/) and NCBI Gene databases (https://www.ncbi.nlm.nih.gov/) (Li et al. 2018).

The standard gene names and UniProt IDs of ACI-related targets were obtained from the UniProtKB database. In the GeneCards database, the probability value derived from a cross-validation analysis was used to rank the targets and estimate the accuracy of the predictions. A probability value $\geq$0.5 was selected in the present study (Gfeller et al. 2014). The database search results were merged, and duplicate targets were deleted to obtain all targets of ACI.

Construction of a Venn diagram

The Venny 2.1 (http://bioinfogp.cnb.csic.es/tools/venny/index.html) online tool was used to map the active ingredients of ZRS and the disease targets to draw Venn diagrams. The intersection of the targeted prediction results of the active components of ZRS and the retrieved results for ACI-related targets was determined, and the common target was selected as the potential therapeutic target of ZRS in the treatment of ACI.

Network model construction and analysis

Protein–protein interactions (PPIs) for each target were generated from the STRING database to help understand cell functions (Szklarczyk et al. 2017). The common targets of the drug and disease were input into the String database (https://string-db.org/cgi/input.pl) to construct the PPI network, and the species was set as '*Homo sapiens*' to obtain the PPI network. The PPI network was imported into Cytoscape 3.6.0 software for a topology analysis and clustering analysis. Degree, betweenness centrality, average shortest path length and closeness centrality were used as the reference standards and sorted by degree. Genes with scores higher than the average were selected as key targets. The MCODE module was used to analyse gene clusters and screen core targets. Based on this information, the component-disease-target network was constructed using Cytoscape 3.8.0 software. The topology analysis of the network was performed, and the components were sorted by degree.

Ingredients with greater than average degree values were selected as the key active ingredients.

GO functional analysis and KEGG pathway enrichment analysis

GO functional enrichment and KEGG pathway analyses were performed on the key targets to explore the main molecular biological processes (BPs) or signalling pathways in which they were involved. The clusterProfiler, enrichplot and ggplot2 packages were installed and used in R 3.6.3 software to generate histograms and bubble plots. The herb-component-disease-pathway-target network was constructed using Cytoscape 3.8.0 software to explore the possible mechanism of action of ZRS in treating ACI.

Molecular docking analysis

In this study, molecular docking analysis was used to determine whether the key targets had good stability with the corresponding active ingredients. The RCSB PDB database (https://www.rcsb.org/) and PubChem database (https://pubchem.ncbi.nlm.nih.gov/) were used to download the stereo structures of core targets and active ingredients. Next, they were preprocessed by PyMol 2.4.0 software. Finally, AutoDock Vina was used to calculate the binding energy according to the hydrogenation reaction between the proteins and small molecule ligands.

Western blot analysis

The extracted brain tissue was lysed and homogenized in RIPA buffer containing protease inhibitors and phosphatase inhibitors. The concentration was determined by performing a BCA protein assay. The proteins were separated on 10% sodium dodecyl sulphate-polyacrylamide gel electrophoresis (SDS-PAGE) gels and then transferred to polyvinylidene fluoride (PVDF) membranes. Subsequently, the membrane was blocked with 5% skim milk powder in blocking solution for 1 h, and the membranes were incubated with the relevant specific antibodies overnight at 4 °C. Then, the membranes were incubated with the corresponding secondary antibody at 37 °C for 2 h. The blots were visualized with ECL reagent. The greyscale values of protein bands were quantified using ImageJ software (Bethesda, MD).

Immunohistochemical analysis

Six rats from per group were used for this analysis. Sections of the infarcted brain were fixed with 4% paraformaldehyde at room temperature for 24 h and then embedded in paraffin. A series of 5 μm thick sections were cut from the block. Paraffin

sections were deparaffinized and hydrated through a series of graded alcohol solutions. Tissue slices were then rinsed with PBS (0.1 M, pH 7.4, 3 × 5 min) and incubated at room temperature with BSA for 30 min. The closure solution was removed, and primary antibody (NF-κB p65 and RAGE) is added dropwise on the sections. Samples were placed flat in a wet box and incubated overnight at 4 °C. The samples were washed with PBS, and corresponding secondary antibodies were added in a dropwise fashion. The samples were incubated at room temperature for 50 min and washed, then DAB chromogenic solution was added. The sample was restained with haematoxylin for 3 min. The nuclei were stained blue with haematoxylin. Positive DAB expression appeared brownish-yellow, and the field of view was selected for image acquisition using a Nikon imaging system (Tokyo, Japan). The result was presented as the positive cell density: number of positive cells/tissue area to be measured.

Statistical analysis

GraphPad Prism 6.0 software (GraphPad Software, Inc., La Jolla, CA) was used for statistical analyses. Data are presented as the means ± SEM. The significance of differences between groups was analysed using one-way ANOVA. $p < 0.05$ was considered to indicate a statistically significant difference.

Results

This study further revealed the mechanism of ZRS action in ACI by combining a network pharmacology analysis and experimental verification, which involves four steps in the workflow shown in Figure 1: (1) TTC staining was performed to verify the cerebral infarct volume in the rats from the three groups, and data were quantitatively analysed. (2) By mining a variety of databases, the components of prescriptions and their corresponding disease-related targets were identified. (3) A multidimensional network graph was constructed and analysed to screen key pathways. (4) The expression levels of related proteins in the key pathways identified above were verified through experiments, and the possible mechanism of the formula in protecting the brain was verified.

ZRS reduces the cerebral infarct volume and improves neurological function

After the MCAO/control operation, the animals were intragastrically administered an equal volume of ZRS or sterile saline for seven days. On day 7 after treatment, neurological function was measured, and brain tissue was collected for TTC staining to determine the infarct size. No obvious lesions were observed in the control group. Compared with the control group, cerebral infarction volume increased significantly after MCAO modelling (58.87%, $p < 0.01$). Compared with the vehicle treatment, ZRS treatment significantly reduced the infarct area in MCAO rats (33.70%, $p < 0.05$) (Figure 2(A,B)). These results suggest that ZRS treatment reduces infarct volume and protects brain tissue in MCAO rats.

Screening of pharmacological targets

By searching the TCMSP database, 259 compound-related targets were identified from the databases after duplicates were eliminated. Among them, 16 active components and 61 targets of *Rheum palmatum* were identified: 93 active components and 2151 targets were obtained from *Radix Glycyrrhiza*, three components and 33 targets were obtained from *Magnoliae officmalis Cortex*, 36 active components and 110 targets were obtained from *Scutellariae Radix*, six active components and 27 targets were obtained from *Radix Vladimiriae*, and 23 active components and 111 targets were obtained from *Fructus aurantii immaturus*.

A total of 2026 related gene targets were retrieved from the GeneCards database, and 112 were retrieved from the NCBI database. After combining and deleting the duplicate genes from the two databases, 2028 ACI-related gene targets were obtained.

Through the intersection of the screened drug targets and disease targets, 187 pharmacological targets of ZRS for the treatment of ACI were identified (Figure 3(A)).

Construction of a PPI network between drugs and ACI and a search for key targets

The 187 common targets obtained in Figure 3(A) were input into the String database for analysis to obtain the PPI network diagram (Figure 3(B)). One hundred and eighty-seven nodes, 3379 edges and an average degree of 40.4 were present in this interaction network.

The PPI network was imported into Cytoscape 3.6.0 software, and a topology analysis was performed using Network Analyzer. Sixty-nine key targets were identified. The first 20 targets were graphed using R 3.6.3 (Figure 3(C)).

The MCODE module was used for gene cluster analysis and core target screening. Ten gene clusters and 10 core genes were obtained, namely, CDK4, RXRA, AR, SREBF1, MMP2, PTGS1, OPRM1, ADRB1, ADRA2C and SLC6A3. The cluster analysis table shows the detailed results (Table 1).

Construction of 'component-disease-target' network and screening of key components

In order to understand the complex interaction among herb, components, diseases and corresponding targets, we established the 'composition-disease-target' network diagram by Cytoscape software. Then, we performed topology analysis for this network structure and found that luteolin (Mol000006), ent-epicatechin (Mol000073), (−)-catechin (Mol000096) and quercetin (Mol000098) were the top four degrees, which indicated that these four components correspond to the largest number of intersecting target (Figure 3(D)). Therefore, these components may be the key components of ZRS for the treatment of ACI. The top 13 active ingredients were screened according to the degree value, as shown in Table 2.

GO functional enrichment and KEGG pathway enrichment analyses

The common targets of drugs and diseases were imported into the STRING database for a gene enrichment analysis (GO) and Kyoto Encyclopedia of Genes and Genomes (KEGG) pathway analysis. A total of 2481 BPs were enriched in the BP category, and the main entries were response to lipopolysaccharide, response to molecules of bacterial origin, cellular response to antibiotic, response to chemical stress, response to nutrient levels, response to reactive oxygen species (ROS), and response to oxidative stress. The cellular component (CC) category revealed enrichment in 170 molecular function (MF)-related items,

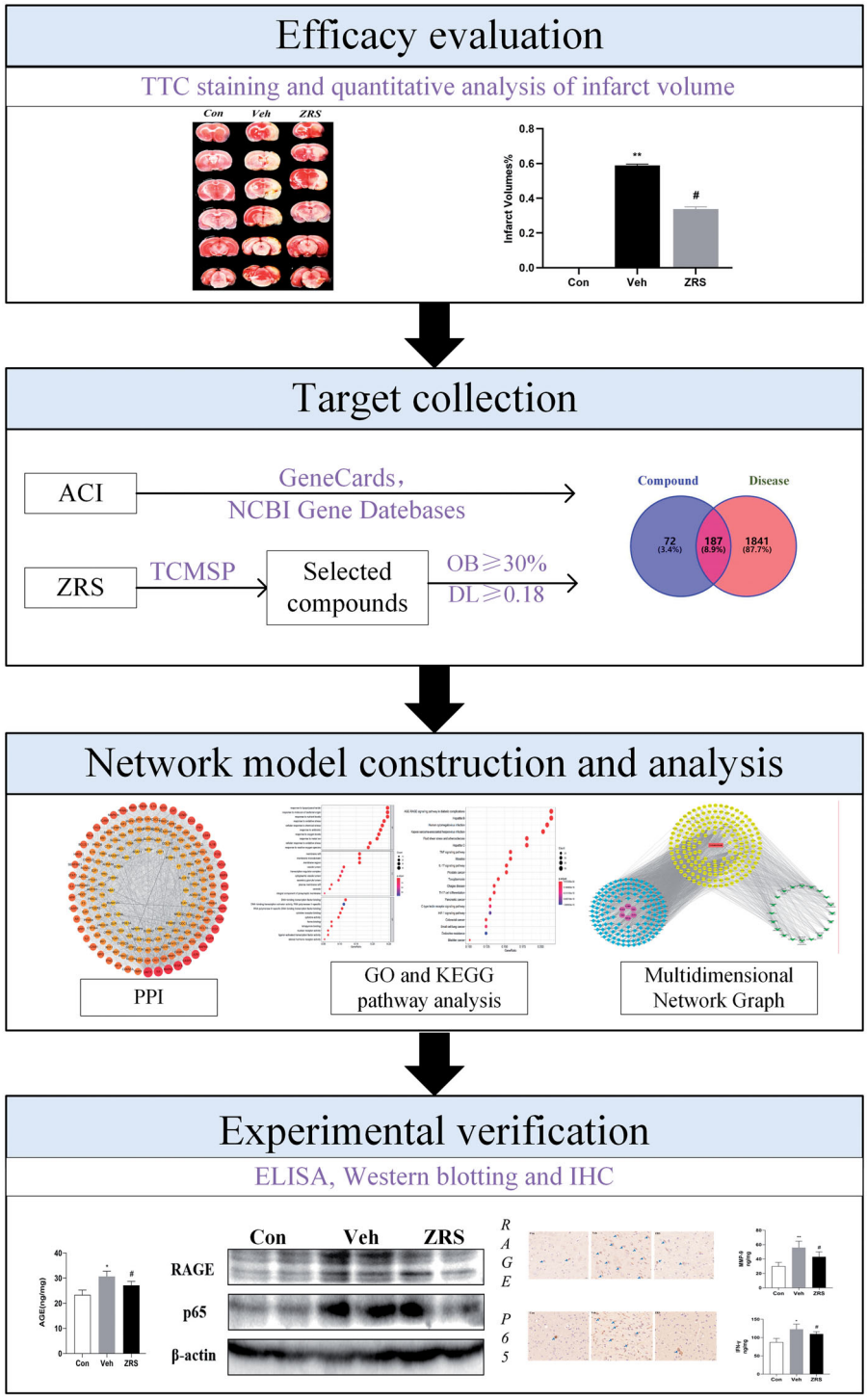

Figure 1. Workflow for cerebral protective effect of ZRS in an MCAO model.

mainly membrane raft, plasma membrane raft, vesicle lumen, integral component of presynaptic membrane, and transcription regulator complex. The MF category showed the enrichment of 94 cell composition-related items, mainly nuclear receptor activity, ligand-activated transcription factor activity, RNA polymerase Il-specific DNA-binding transcription factor binding, cytokine activity, DNA-binding transcription factor binding and heme binding (Figure 4(A)).

The KEGG pathway analysis indicated 169 enriched signalling pathways, and the results are shown in Figure 4(B). These enriched pathways mainly included the AGE-RAGE signalling pathway in diabetic complications, IL-17 signalling pathway, TNF signalling pathway, Th17 cell differentiation, C-type lectin receptor signalling pathway and HIF-1 signalling pathway.

Multidimensional network graph analysis

The drugs, diseases, active ingredients, key targets and KEGG pathway information described above were used to construct a multidimensional network diagram, and the relationship between the herb-chemical composition-core target-disease-key pathway

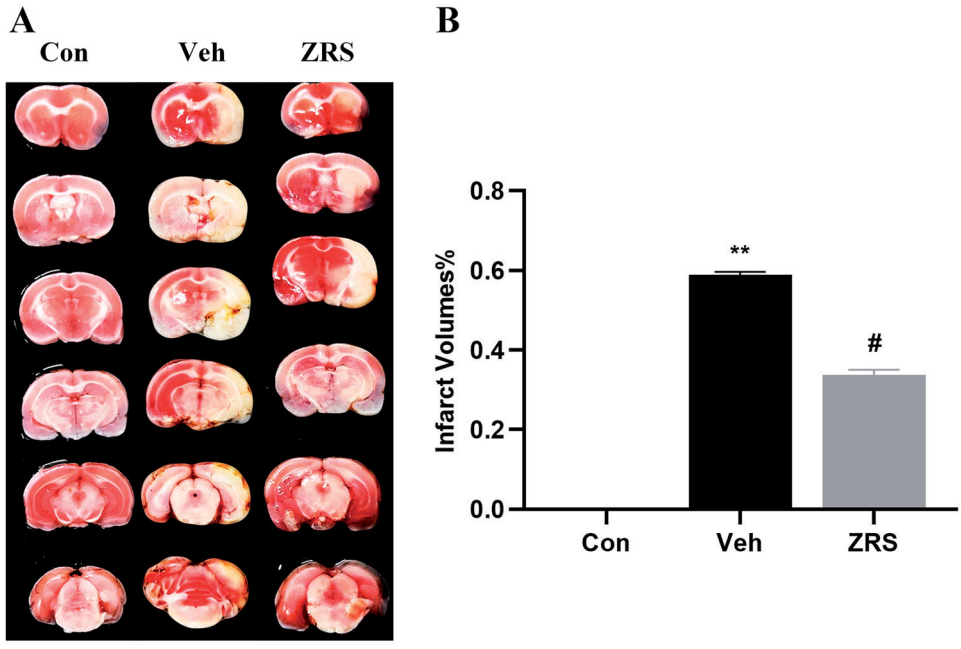

Figure 2. Effects of ZRS on the infarct volume in MCAO rats. (A) The effect of ZRS on the infarct size was measured by performing TTC staining. After TTC staining of the brain, the lesions appeared as white areas. Samples from the ZRS treatment group had smaller lesions than those from the vehicle group. No obvious lesions were observed in the control group. (B) Quantitative analysis of the infarct volume in rat brain tissue. Control vs. vehicle, $^{**}p < 0.01$; ZRS vs. vehicle, $^{\#}p < 0.05$, $n = 6$ rats per group, means ± SEM.

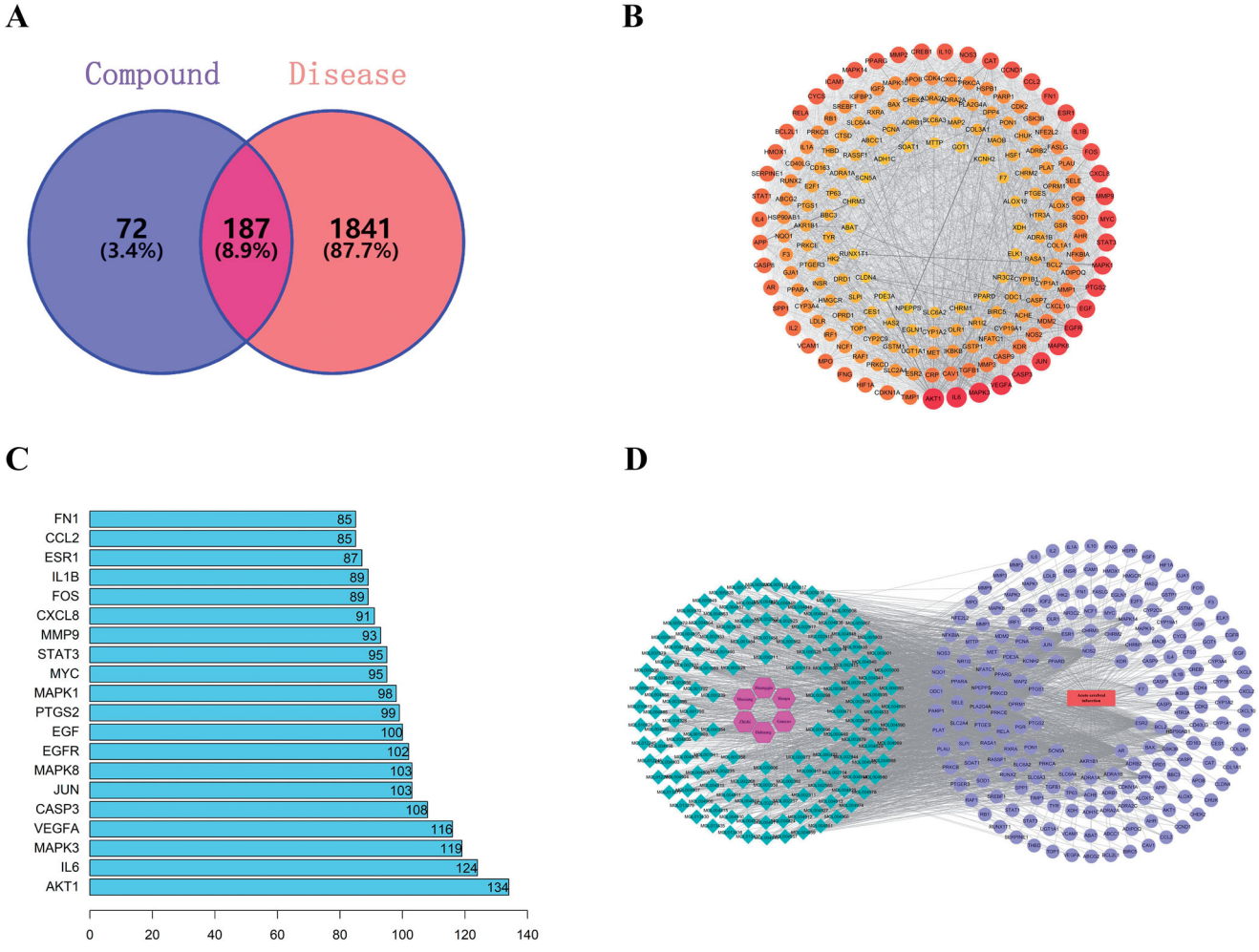

Figure 3. Network construction and analysis. (A) Wayne figure. The intersection of ZRS targets and disease targets. One hundred and eighty-seven targets were shared by ZRS and ACI. (B) A PPI network diagram was drawn using Cytoscape software. The colour and size of the nodes were adjusted according to the degree value, and the thickness of the line indicates that the edge betweenness ranges from large to small. (C) The ranking of ZRS target importance for treating ACI. The abscissa is the degree value of each target. (D) Component-disease-target Network. In the network, the circle is the target of drugs acting on diseases, the rhombus is compound, the hexagon is herb, and the rectangle is disease.

Table 1. MCODE cluster analysis.

Cluster	Score	Nodes	Edges	Node IDs
1	47.107	57	1319	VCAM1, IL2, CXCL10, SERPINE1, PLAU, SPP1, ESR1, MAPK8, EGF, EGFR, MMP2, FOS, JUN, CASP3, TGFB1, CASP8, CREB1, NOS3, AKT1, SELE, CDKN1A, ADIPOQ, CCND1, KDR, VEGFA, MMP1, MAPK14, MAPK3, CRP, CCL2, MPO, IL4, HMOX1, CXCL8, MYC, MAPK1, PTGS2, CAT, ICAM1, PPARG, IL6, IL10, TIMP1, MMP9, CD40LG, IL1B, CYCS, CASP9, STAT3, FASLG, FN1, RELA, IFNG, STAT1, MMP3, BCL2L1, HIF1A
2	6.571	8	23	RXRA, NR1I2, CYP3A4, CYP1A2, UGT1A1, CYP1B1, CYP2C9, CYP1A1
3	4.842	20	46	IL1A, NFKBIA, APP, NOS2, MET, CAV1, RUNX2, SOD1, MDM2, NCF1, MAPK10, CDK2, CXCL2, AR, PGR, HSPB1, GJA1, NFATC1, AHR, NFE2L2
4	4	5	8	DPP4, SLC2A4, SREBF1, APOB, PPARA
5	4	5	8	DRD1, ADRB1, SLC6A4, HTR3A, ADRA1B
6	3.5	5	7	OPRM1, ADRB2, CHRM2, ACHE, OPRD1
7	3.5	5	7	ADRA2C, ADRA2A, MAP2, PTGER3, PRKCE
8	3.077	14	20	PARP1, CYP19A1, CDK4, THBD, ABCG2, LDLR, GSK3B, RB1, IGFBP3, PLAT, IGF2, ESR2, CASP7, CD163
9	3	3	3	PTGES, PTGS1, PLA2G4A
10	3	5	6	ADRA1A, MAOB, CHRM1, SLC6A3, CHRM3

Table 2. Basic information of 13 active ingredients in ZRS.

Mol ID	Molecule name	Average shortest path length	Betweenness centrality	Closeness centrality	Degree
MOL000006	Luteolin	1.89583333	0.13686719	0.52747253	133
MOL000073	*ent*-Epicatechin	2.33630952	0.02356187	0.42802548	59
MOL000096	(–)-Catechin	2.38392857	0.01446247	0.41947566	47
MOL000098	Quercetin	2.33630952	0.02444688	0.42802548	45
MOL000173	Wogonin	2.42559524	0.00430319	0.41226994	40
MOL000211	Mairin	2.4077381	0.01044336	0.41532756	39
MOL000228	(2*R*)-7-Hydroxy-5-methoxy-2-phenylchroman-4-one	2.44940476	0.00354751	0.40826245	37
MOL000239	Jaranol	2.44345238	0.00498223	0.409257	37
MOL000354	Isorhamnetin	2.44345238	0.00609192	0.409257	35
MOL000358	β-Sitosterol	2.46130952	0.00315074	0.40628779	34
MOL000359	Sitosterol	2.45535714	0.00180895	0.40727273	33
MOL000392	Formononetin	2.4672619	0.0012854	0.4053076	32
MOL000417	Calycosin	2.4672619	0.00116801	0.4053076	32

was obtained from the interactions among nodes of the multidimensional network diagram, as shown in Figure 4(C). ZRS may ameliorate the brain injury caused by ACI through multiple pathways and multiple targets. The AGE-RAGE pathway may be an important signalling pathway in ZRS-mediated treatment of ACI.

Molecular docking between core targets and active ingredients

Binding energy is considered to be one of the key indicators to verify the stability of the conformation of the bound protein and active ingredient (Sun et al. 2022). Therefore, we performed molecular docking analysis on the top 5 key target and the top 4 bioactive components, and the results are shown in Figure 5. According to the results, the binding energy of the analysed active ingredients and targets were all lower than −5.0 kcal/mol (Figure 5(A), Table 3), which reflected that ZRS plays a role in the treatment of ACI through multiple targets. In addition, we found that luteolin, the most important bioactive component of ZRS, obtained the highest binding energy of 9.4 kcal/mol for binding to the protein AKT1. Similarly, the highest binding energy of 9.2 kcal/mol was obtained for ent-epicatechin binding to AKT1, and the binding energies of (–)-catechin and quercetin to AKT1 were 9.4 kcal/mol. Moreover, we showed the strongest binding active structure of the interaction between each bioactive ingredient and the key protein with the strongest binding activity (Figure 5(B)).

ZRS reduces neuroinflammation by inhibiting the activation of the AGE-RAGE pathway after ACI

ELISA, Western blotting and IHC were used to detect the changes in AGE-RAGE pathway-related proteins. The ELISA results indicated increased levels of AGEs after ACI, and ZRS reduced the AGE levels. Similarly, the Western blotting and IHC results showed that the levels of RAGE and NF-κB p65 were increased in the MCAO group, but ZRS reversed these changes. Based on this finding, the AGE-RAGE pathway was activated by ACI, whereas ZRS inhibited the activation of this pathway (Figure 6(A–H)).

The AGE-RAGE signalling pathway was activated after ACI, which led to subsequent neuroinflammation. Thus, we measured the release of inflammatory cytokines. The expression levels of IFN-γ and MMP-9 in the ischaemic brain were significantly increased, and ZRS effectively inhibited the release of these inflammatory molecules (Figure 6(I,J)).

Discussion

Acute stroke has a high disability rate and limited treatment options (Shekhar et al. 2018). Inflammation is presumed to play an important role in the ischaemic stroke process (Chen et al. 2020). After cerebral ischaemia, the immune system is activated to generate a sterile inflammatory response, leading to the production of chemokines and cytokines and the infiltration of white blood cells in the ischaemic tissue. Finally, microvascular damage and BBB damage occur, which aggravate brain injury (De-Meyer et al. 2016; Jayaraj et al. 2019). According to recent

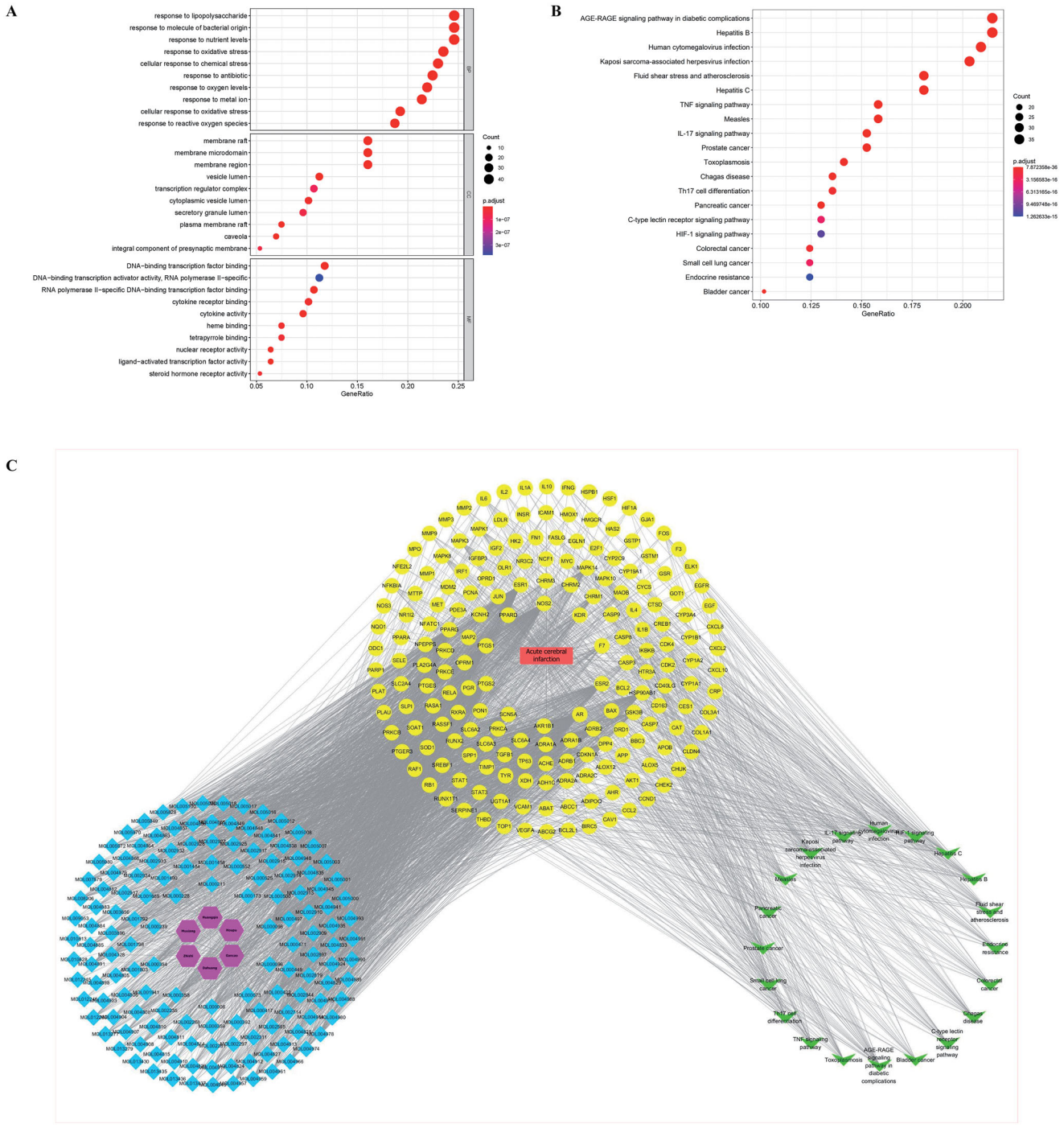

Figure 4. Network pharmacology prediction of ZRS treatment for ACI. (A) Results of the GO enrichment analysis. Dot plots show the top 10 terms in the BP, CC and MF categories from the GO analysis; the abscissa corresponds to the number of genes annotated, the ordinate represents the GO term, the size of the dots corresponds to the count of genes annotated in the entry, and the colour of the dots corresponds to the corrected *p* value. (B) Results of the KEGG enrichment analysis. (C) The herb-chemical composition-core target-disease-key pathway multilevel network. Purple represents the herb, blue represents the active ingredient of the herb, yellow represents the target of ZRS acting on the disease, green represents the top 20 most significant pathways, and red represents the disease, namely, acute cerebral infarction.

studies, 50% of patients with stroke will experience gastrointestinal complications, which might decrease the regulatory effect of the central nervous system (CNS) on the enteric nervous system (ENS) due to the inhibition of cerebral cortical function (Wen and Wong 2017). Gastrointestinal dysfunction results in impaired function of the intestinal barrier system. A large number of inflammatory mediators are released into the blood, leading to a systemic inflammatory response (Yoo et al. 2020) that is not conducive to the recovery of nervous system function. In China, traditional Chinese medicine has been used to treat stroke for thousands of years (Shang et al. 2015). According to the theory of traditional Chinese medicine, acute stroke is associated with heat-phlegm and sthenic-fu (Wu et al. 2017), and thus the treatment is mainly based on the method of purging fu-

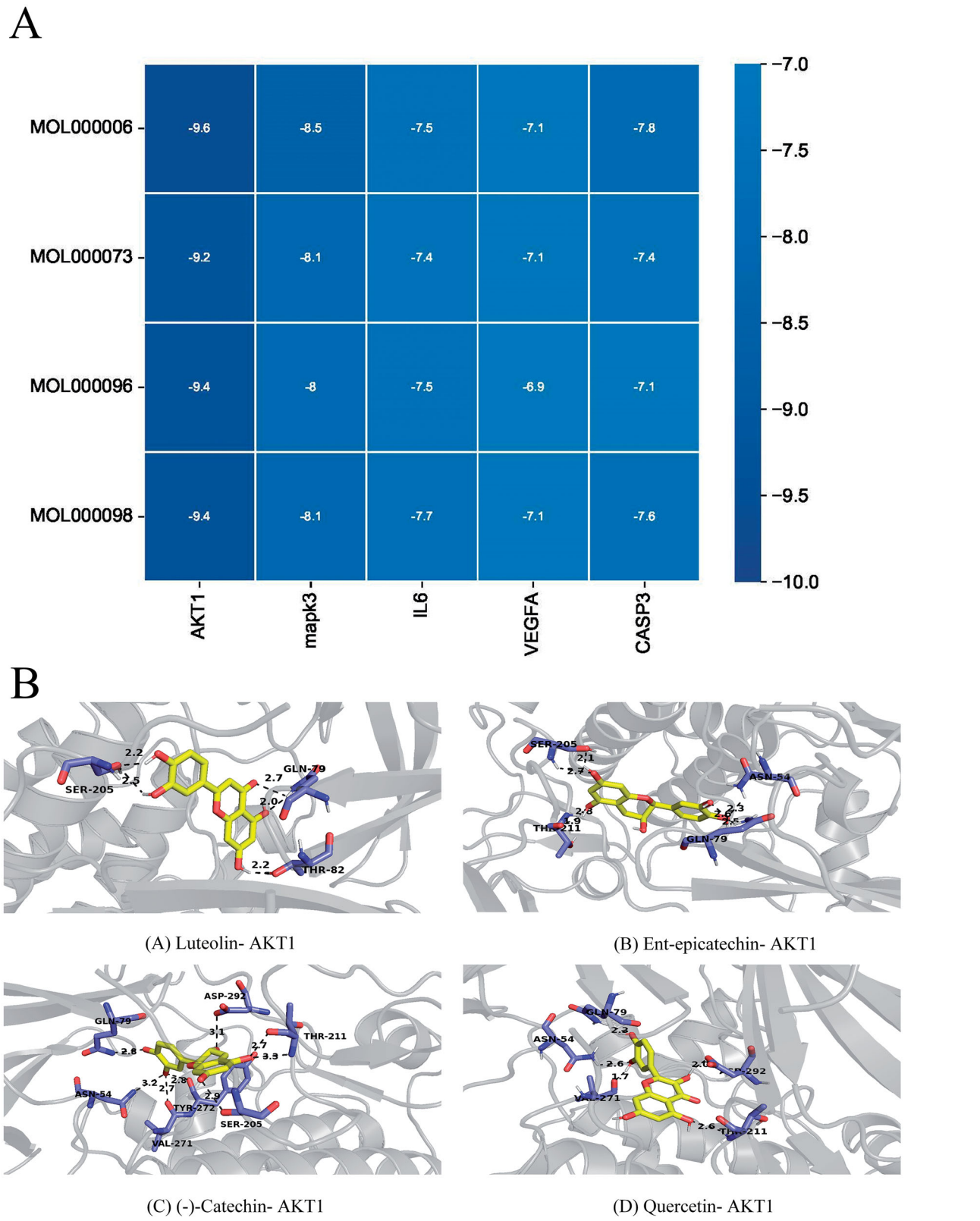

Figure 5. Molecular docking between core targets and active ingredients. (A) Heat map of binding energy between five core targets and top four active ingredients by molecular docking. (B) Four conformation examples of some core compounds and key targets. (A) Luteolin – AKT1, (B) *ent*-Epicatechin – AKT1, (C) (–)-catechin – AKT1 and (D) quercetin – AKT1.

organ. The effect of Zhishi Rhubarb Soup (ZRS) is to reduce phlegm and mediate qi, which positively improves the symptoms related to ACI.

The efficacy of a Chinese herbal decoction is based on the synergistic effects of many components, targets and pathways (Yuan et al. 2017). Network pharmacology has recently been

Table 3. Binding energy values of the key ingredient in ZRS with core targets.

Core components MolName	Core targets				
	AKT1	MAPK3	IL6	VEGFA	CASP3
MOL000006	−9.6	−8.5	−7.5	−7.1	−7.8
MOL000073	−9.2	−8.1	−7.4	−7.1	−7.4
MOL000096	−9.4	−8	−7.5	−6.9	−7.1
MOL000098	−9.4	−8.1	−7.7	−7.1	−7.6

applied to determine the compatibility of complex traditional Chinese medicine prescriptions (Jarrell et al. 2018). In the present study, a multidimensional network map was constructed using a network pharmacology method to identify the key compounds and key targets of ZRS in the treatment of ACI. In the next step, the mechanism of action of ZRS was assessed by performing Gene Ontology (GO) and the KEGG enrichment

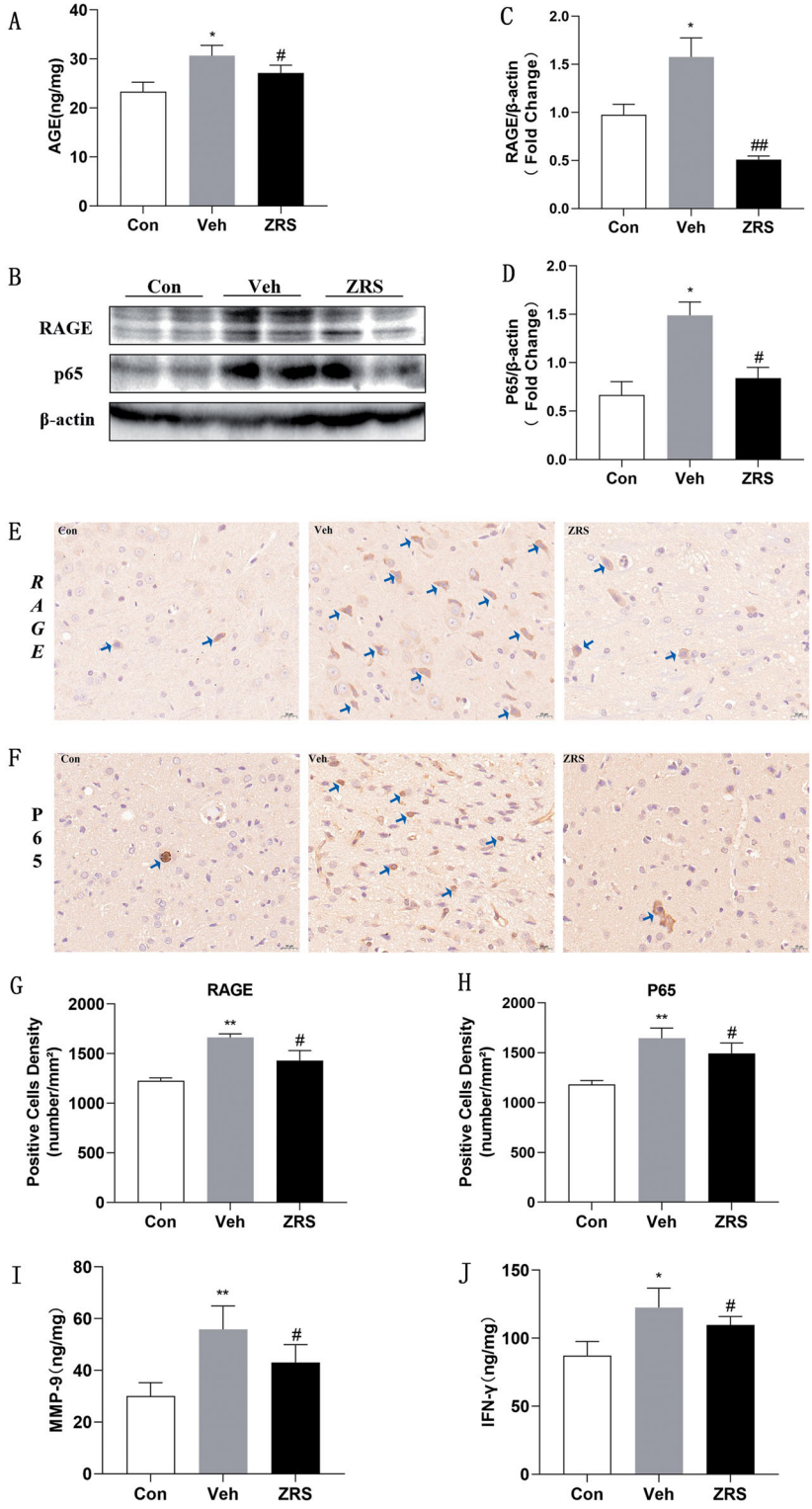

Figure 6. Effects of ZRS on the AGE-RAGE signalling pathway and downstream inflammatory cytokine activation after ACI. (A) Serum AGE levels measured using ELISA. (B) Representative images of RAGE and p65 levels detected using Western blotting. (C, D) The greyscale results for RAGE and P65 (/β-actin) levels. (E, F) Representative images of IHC staining for RAGE and p65 (×40; the arrow identifies a positive cell). (G, H) Positive expression of RAGE and P65. (I) Serum levels of MMP-9 detected using an ELISA. (J) Serum levels of IFN-γ detected using an ELISA. Control vs. vehicle, $^{*}p < 0.05$ and $^{**}p < 0.01$; ZRS vs. vehicle, $^{\#}p < 0.05$ and $^{\#\#}p < 0.01$, $n = 6$ rats per group, means ± SEM.

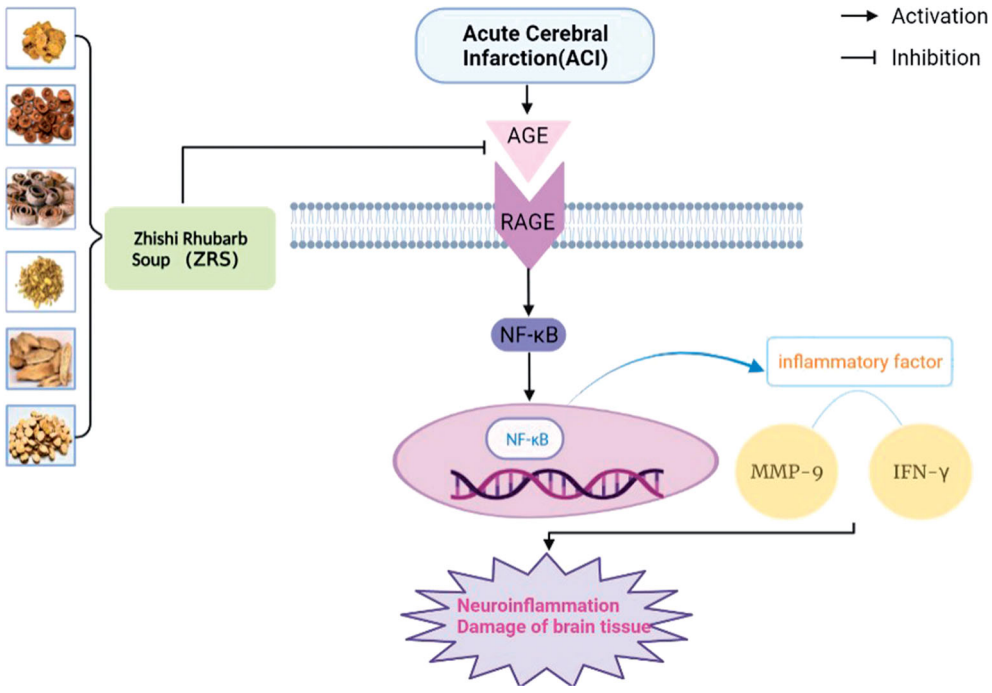

Figure 7. Schematic diagram of the protective effect of ZRS on ischaemic brain tissue by blocking the AGE-RAGE-NF-κB signalling pathway. After ischaemic stroke, AGE levels are increased, and the binding of AGEs to their receptor RAGE activates the NF-κB signalling pathway. NF-κB activation promotes the expression of inflammatory factors such as IFN-γ and MMP-9, thereby exacerbating brain injury. However, ZRS inhibits neuroinflammation and alleviates brain injury by inhibiting the AGE-RAGE-NF-κB signalling pathway after ischaemic stroke.

analyses. In combination with subsequent animal experiments, the complex interaction between Chinese herbs in the prescription was discussed, and the mechanism of action of ZRS in the treatment of ACI was explored.

Following network construction and the central network topology analysis, 69 key targets were selected, including AKT1, IL-6, MAPK, VEGFA and CASP3. The network topology analysis showed that ZRS treatment for ACI was a complex process involving multiple BPs, cell components and MFs. Enrichment analyses showed that the effective components of ZRS played a role in the treatment of ACI mainly by modulating the AGE-RAGE signalling pathway, hepatitis B, IL-17 signalling pathway, hepatitis C, human cytomegalovirus infection, TNF signalling pathway, Th17 cell differentiation, C-type lectin receptor signalling pathway and HIF-1 signalling pathway, among others.

Among these pathways predicted by network pharmacology, studies have shown that the AGEs/RAGE/NF-κB signalling pathway plays an important role in oxidative stress and excessive inflammation (Yu et al. 2018). Advanced glycation end products (AGEs) were previously reported to exert a proinflammatory effect (Subedi et al. 2020); inflammation plays an important role in cerebral ischaemia injury (Chen et al. 2020). The interaction between AGEs and their receptor RAGE leads to the production of ROS and damage to the BBB, which exacerbate neuroinflammation and neurodegeneration (Yang et al. 2015; Sanajou et al. 2018). Previous studies have suggested that RAGE may cause delayed neuronal death after global cerebral ischaemia by exacerbating vascular injury and harmful glia-mediated inflammation (Kamide et al. 2012). In addition, the binding of AGEs to RAGE on macrophages activates several signal transduction pathways, such as P21RAS, MAPK and PI3K/Akt. These signals eventually lead to oxidative stress and NF-κB activation (Singh et al. 2014). In the resting state of the cell, NF-κB usually forms a dimer of NF-κB P65/P50 bound to the NF-κB inhibitory protein (IκB) in the cytoplasm (Cai et al. 2020). When cells are exposed to proinflammatory signals (e.g., cytokines and pathogens), the phosphorylation and hydrolysis of IκB result in the separation of NF-κB from this inhibitory protein and activation (Giridharan and Srinivasan 2018). NF-κB regulates the expression of several genes, including MMP-9 and IFN-γ, which are involved in inflammation (Li et al. 2017; Lu et al. 2018). Our study confirmed significantly increased expression levels of AGE, RAGE and NF-κB P65 after ACI and decreases after ZRS administration, revealing that ZRS inhibited the ACI-induced activation of the AGE-RAGE signalling pathway.

Interferon-γ (IFN-γ) is an important inflammatory mediator involved in inflammation and the immune response after cerebral ischaemia injury (Wang et al. 2020). IFN-γ promotes leukocyte adhesion and may promote tissue necrosis and nerve dysfunction (Yilmaz et al. 2006). In addition, infiltrating leukocytes may increase the expression of MMP-9. MMP-9 is the most widely studied enzyme in acute ischaemic stroke because it disrupts the BBB by degrading tight junctions and basal lamina proteins, thereby triggering subsequent inflammatory responses (Kawabori and Yenari 2015). In the present study, the serum levels of IFN-γ and MMP-9 in the MCAO model are significantly increased, and ZRS reduced the levels of these inflammatory factors. Based on these results, ZRS may play a neuroprotective role that is possibly mediated by its anti-inflammatory effect.

ZRS exerts a significant therapeutic effect on ACI, and its mechanism may be related to the blockade of the AGEs/RAGE/NF-κB signalling pathway and the subsequent decrease in the expression of the downstream mediators IFN-γ and MMP-9 (Figure 7). Despite the positive results observed, this study has some limitations. First, this study focussed on the neuroinflammatory response as one of the important underlying mechanisms of the neuroprotective effect of ZRS on cerebral ischaemia. However, based on the multiple components, targets and pathways of TCM compounds, other related mechanisms, such as oxidative stress, apoptosis, mitochondrial function and

autophagy, have not been elucidated, and thus further studies are needed to verify them in the future. In addition, AGE-RAGE pathway activation may lead to the activation of downstream pathways, including JAK-STAT, MAPK/ERK and PI3K/Akt/MTOR. The common end point for these pathways is the activation of nuclear transcription factors involved in inflammatory and fibrotic processes (Sanajou et al. 2018), which mediate brain damage after stroke by regulating oxidative stress responses, neuroinflammation and apoptosis. In the future, we plan to further study the related indicators of this pathway by performing *in vitro* experiments and animal experiments.

Conclusions

By combining network pharmacology and animal experiments, this research project systematically and comprehensively investigated the ZRS mechanism in the treatment of ACI and clarified the synergistic multicomponent and multitarget mechanism of ZRS for the first time. Meanwhile, we verified that ZRS reduces neuroinflammation by inhibiting the activation of the AGE-RAGE pathway, thus exerting a protective effect on rat brain tissue.

Consent form

All named authors have agreed to the publication of the work.

Author contributions

JHZ and YJS contributed to the conception and design of the study; YJS, YZ, RRW and LRD performed the experiments and analysed the data; YJS wrote the initial draft of the manuscript; JHZ revised the manuscript; YJS, FJC and YQY created and arranged the figures; CH, YZ and JHZ arranged the study funds; and all authors contributed to manuscript revision and read and approved the submitted version.

Disclosure statement

The authors report no declarations of interest.

Funding

The research is financially supported by the Nanjing Municipal Health Commission Fund Project (Grant Number YKK19098), Nanjing TCM Youth Talent Training Program (Grant Number ZYQ20004) and Jiangsu Province Graduate Experimental Innovation Plan in 2022 (Grant Number SJCX22-0821).

Data availability statement

The data that support the findings of this study are available from the corresponding author upon reasonable request.

References

Albers GW, Marks MP, Kemp S, Christensen S, Tsai JP, Ortega-Gutierrez S, McTaggart RA, Torbey MT, Kim-Tenser M, Leslie-Mazwi T, et al. 2018. Thrombectomy for stroke at 6 to 16 hours with selection by perfusion imaging. N Engl J Med. 378(8):708–718.

Anderson CS, Huang Y, Lindley RI, Chen X, Arima H, Chen G, Li Q, Billot L, Delcourt C, Bath PM, et al. 2019. Intensive blood pressure reduction with intravenous thrombolysis therapy for acute ischaemic stroke (ENCHANTED): an international, randomised, open-label, blinded-endpoint, phase 3 trial. Lancet. 393(10174):877–888.

Cai M, Liao Z, Zou X, Xu Z, Wang Y, Li T, Li Y, Ou X, Deng Y, Guo Y, et al. 2020. Herpes simplex virus 1 UL2 inhibits the TNF-α-mediated NF-κB activity by interacting with p65/p50. Front Immunol. 11:549.

Chen X, Chen H, He Y, Fu S, Liu H, Wang Q, Shen J. 2020. Proteomics-guided study on Buyang Huanwu decoction for its neuroprotective and neurogenic mechanisms for transient ischemic stroke: involvements of EGFR/PI3K/Akt/Bad/14-3-3 and Jak2/Stat3/cyclin D1 signaling cascades. Mol Neurobiol. 57(10):4305–4321.

Chen H, He Y, Chen S, Qi S, Shen J. 2020. Therapeutic targets of oxidative/nitrosative stress and neuroinflammation in ischemic stroke: applications for natural product efficacy with omics and systemic biology. Pharmacol Res. 158:104877.

De-Meyer SF, Denorme F, Langhauser F, Geuss E, Fluri F, Kleinschnitz C. 2016. Thromboinflammation in stroke brain damage. Stroke. 47(4):1165–1172.

Engel O, Kolodziej S, Dirnagl U, Prinz V. 2011. Modeling stroke in mice – middle cerebral artery occlusion with the filament model. J Vis Exp. 47:2423.

George PM, Steinberg GK. 2015. Novel stroke therapeutics: unraveling stroke pathophysiology and its impact on clinical treatments. Neuron. 87(2):297–309.

Gfeller D, Grosdidier A, Wirth M, Daina A, Michielin O, Zoete V. 2014. Swiss Target Prediction: a web server for target prediction of bioactive small molecules. Nucleic Acids Res. 42(Web Server issue):W32–W38.

Giridharan S, Srinivasan M. 2018. Mechanisms of NF-κB p65 and strategies for therapeutic manipulation. J Inflamm Res. 11:407–419.

He J, Liu J, Huang Y, Tang X, Xiao H, Hu Z. 2021. Oxidative stress, inflammation, and autophagy: potential targets of mesenchymal stem cells-based therapies in ischemic stroke. Front Neurosci. 15:641157.

Iadecola C, Anrather J. 2011. The immunology of stroke: from mechanisms to translation. Nat Med. 17(7):796–808.

Jarrell JT, Gao L, Cohen DS, Huang X. 2018. Network medicine for Alzheimer's disease and traditional Chinese medicine. Molecules. 23(5):1143.

Jayaraj RL, Azimullah S, Beiram R, Jalal FY, Rosenberg GA. 2019. Neuroinflammation: friend and foe for ischemic stroke. J Neuroinflammation. 16(1):142.

Jiao X, Jin X, Ma Y, Yang Y, Li J, Liang L, Liu R, Li Z. 2021. A comprehensive application: molecular docking and network pharmacology for the prediction of bioactive constituents and elucidation of mechanisms of action in component-based Chinese medicine. Comput Biol Chem. 90:107402.

Jones KA, Maltby S, Plank MW, Kluge M, Nilsson M, Foster PS, Walker FR. 2018. Peripheral immune cells infiltrate into sites of secondary neurodegeneration after ischemic stroke. Brain Behav Immun. 67:299–307.

Kamide T, Kitao Y, Takeichi T, Okada A, Mohri H, Schmidt AM, Kawano T, Munesue S, Yamamoto Y, Yamamoto H, et al. 2012. RAGE mediates vascular injury and inflammation after global cerebral ischemia. Neurochem Int. 60(3):220–228.

Kawabori M, Yenari MA. 2015. Inflammatory responses in brain ischemia. Curr Med Chem. 22(10):1258–1277.

Kong LL, Wang ZY, Han N, Zhuang XM, Wang ZZ, Li H, Chen NH. 2014. Neutralization of chemokine-like factor 1, a novel C-C chemokine, protects against focal cerebral ischemia by inhibiting neutrophil infiltration via MAPK pathways in rats. J Neuroinflammation. 11:112.

Lansberg MG, Bluhmki E, Thijs VN. 2009. Efficacy and safety of tissue plasminogen activator 3 to 4.5 hours after acute ischemic stroke: a metaanalysis. Stroke. 40(7):2438–2441.

Li W, Suwanwela NC, Patumraj S. 2017. Curcumin prevents reperfusion injury following ischemic stroke in rats via inhibition of NF-κB, ICAM-1, MMP-9 and caspase-3 expression. Mol Med Rep. 16(4):4710–4720.

Li YH, Yu CY, Li XX, Zhang P, Tang J, Yang Q, Fu T, Zhang X, Cui X, Tu G, et al. 2018. Therapeutic target database update 2018: enriched resource for facilitating bench-to-clinic research of targeted therapeutics. Nucleic Acids Res. 46(D1):D1121–D1127.

Liu H, Chen X, Liu Y, Fang C, Chen S. 2021. Antithrombotic effects of Huanglian Jiedu decoction in a rat model of ischaemia–reperfusion-induced cerebral stroke. Pharm Biol. 59:823–827.

Lu Y, Yang YY, Zhou MW, Liu N, Xing HY, Liu XX, Li F. 2018. Ketogenic diet attenuates oxidative stress and inflammation after spinal cord injury by activating Nrf2 and suppressing the NF-κB signaling pathways. Neurosci Lett. 683:13–18.

Lv S, Zhang JH, Cao FJ, Sheng L, Yu HM. 2022. Effect of modified Zhishi Dahuang decoction on patients with acute ischemic stroke (phlegm heat and fu stagnation syndrome). J Tradit Chin Med. 31(5):847–850.
Mo Z, Tang C, Li H, Lei J, Zhu L, Kou L, Li H, Luo S, Li C, Chen W, et al. 2020. Eicosapentaenoic acid prevents inflammation induced by acute cerebral infarction through inhibition of NLRP3 inflammasome activation. Life Sci. 242:117133.
Ovbiagele B, Nguyen-Huynh MN. 2011. Stroke epidemiology: advancing our understanding of disease mechanism and therapy. Neurotherapeutics. 8(3):319–329.
Rabinstein AA. 2017. Treatment of acute ischemic stroke. Continuum. 23(1): 62–81.
Ru J, Li P, Wang J, Zhou W, Li B, Huang C, Li P, Guo Z, Tao W, Yang Y, et al. 2014. TCMSP: a database of systems pharmacology for drug discovery from herbal medicines. J Cheminform. 6:13.
Sanajou D, Ghorbani Haghjo A, Argani H, Aslani S. 2018. AGE-RAGE axis blockade in diabetic nephropathy: current status and future directions. Eur J Pharmacol. 833:158–164.
Shang LX, Liang ZL, Zhang HL. 2015. Relationship between syndrome differentiation and serum inflammatory factors of acute ischemic stroke (middle meridian). J Emerg Tradit Chin Med. 24:329–331.
Shekhar S, Cunningham MW, Pabbidi MR, Wang S, Booz GW, Fan F. 2018. Targeting vascular inflammation in ischemic stroke: recent developments on novel immunomodulatory approaches. Eur J Pharmacol. 833:531–544.
Singh VP, Bali A, Singh N, Jaggi AS. 2014. Advanced glycation end products and diabetic complications. Korean J Physiol Pharmacol. 18(1):1–14.
Subedi L, Lee JH, Gaire BP, Kim SY. 2020. Sulforaphane inhibits MGO-AGE-Mediated neuroinflammation by suppressing NF-κB, MAPK, and AGE-RAGE signaling pathways in microglial cells. Antioxidants. 9:792.
Sun W, Chen Y, Li M. 2022. Systematic elaboration of the pharmacological targets and potential mechanisms of ZhiKe GanCao decoction for preventing and delaying intervertebral disc degeneration. Evid Based Complement Alternat Med. 2022:8786052.
Szklarczyk D, Morris JH, Cook H, Kuhn M, Wyder S, Simonovic M, Santos A, Doncheva NT, Roth A, Bork P, et al. 2017. The STRING database in 2017: quality-controlled protein-protein association networks, made broadly accessible. Nucleic Acids Res. 45(D1):D362–D368.
Wang Y, Xiao G, He S, Liu X, Zhu L, Yang X, Zhang Y, Orgah J, Feng Y, Wang X, et al. 2020. Protection against acute cerebral ischemia/reperfusion injury by QiShenYiQi via neuroinflammatory network mobilization. Biomed Pharmacother. 125:109945.
Wen SW, Wong C. 2017. An unexplored brain-gut microbiota axis in stroke. Gut Microbes. 8(6):601–606.
Wu S, Chen P, Jiang L. 2017. Correlation analysis of symptom elements and signs of terombelastogram in acute ischemic stroke patients with phlegm-heat and bowel-qi-obstructed syndrome. Chin J Integr Med Cardio Cerebrovasc Dis. 15:2966–2968.
Xu M, Wu RX, Li XL, Zeng YS, Liang JY, Fu K, Liang Y, Wang Z. 2022. Traditional medicine in China for ischemic stroke: bioactive components, pharmacology, and mechanisms. J Integr Neurosci. 21(1):26.
Yang L, Qian J, Yang B, He Q, Wang J, Weng Q. 2021. Challenges and improvements of novel therapies for ischemic stroke. Front Pharmacol. 12:721156.
Yang F, Wang Z, Zhang JH, Tang J, Liu X, Tan L, Huang QY, Feng H. 2015. Receptor for advanced glycation end-product antagonist reduces blood–brain barrier damage after intracerebral hemorrhage. Stroke. 46(5): 1328–1336.
Yilmaz G, Arumugam TV, Stokes KY, Granger DN. 2006. Role of T lymphocytes and interferon-gamma in ischemic stroke. Circulation. 113(17): 2105–2112.
Yoo JY, Groer M, Dutra S, Sarkar A, McSkimming DI. 2020. Gut microbiota and immune system interactions. Microorganisms. 8(10):1587.
Yu W, Tao M, Zhao Y, Hu X, Wang M. 2018. 4′-Methoxyresveratrol alleviated AGE-induced inflammation via RAGE-mediated NF-κB and NLRP3 inflammasome pathway. Molecules. 23(6):1447.
Yuan H, Ma Q, Cui H, Liu G, Zhao X, Li W, Piao G. 2017. How can synergism of traditional medicines benefit from network pharmacology? Molecules. 22(7):1135.
Zeng Q, Li L, Siu W, Jin Y, Cao M, Li W, Chen J, Cong W, Ma M, Chen K, et al. 2019. A combined molecular biology and network pharmacology approach to investigate the multi-target mechanisms of Chaihu Shugan San on Alzheimer's disease. Biomed Pharmacother. 120:109370.
Zhang JH. 2019. Zhang Zhongai's experience in treating for acute stroke with TCM TiaoqiTongfu method. Acta Chin Med. 34:303–306.
Zhang JH, Hui Z, Wang SL, Huang C, Zhao Y. 2021. Effects of Jiajian Zhishi Rhubarb Soup on inflammatory factors and TXB2, 6-keto-PGF1α contents in MCAO model rats. Lishizhen Med Mater Med Res. 32(01):21–23.
Zhang JH, Shao YJ, Hui Z, Wang SL, Huang C, Zhao Y. 2021. The proteomics analysis of the effects of Zhishi Rhubarb Soup on ischaemic stroke. Proteome Sci. 19(1):13.
Zhang W, Zhang L, Wang WJ, Ma S, Wang M, Yao M, Li R, Li WW, Zhao X, Hu D, et al. 2022. Network pharmacology and *in vitro* experimental verification to explore the mechanism of Sanhua decoction in the treatment of ischaemic stroke. Pharm Biol. 60(1):119–130.
Zhao S, Liu Z, Wang M, He D, Liu L, Shu Y, Song Z, Li H, Liu Y, Lu A. 2018. Anti-inflammatory effects of Zhishi and Zhiqiao revealed by network pharmacology integrated with molecular mechanism and metabolomics studies. Phytomedicine. 50:61–72.
Zhao GC, Yuan YL, Chai FR, Ji FJ. 2017. Effect of *Melilotus officinalis* extract on the apoptosis of brain tissues by altering cerebral thrombosis and inflammatory mediators in acute cerebral ischemia. Biomed Pharmacother. 89:1346–1352.
Zhuang T, Gu X, Zhou N, Ding L, Yang L, Zhou M. 2020. Hepatoprotection and hepatotoxicity of Chinese herb rhubarb (dahuang): how to properly control the "general (jiang jun)" in Chinese medical herb. Biomed Pharmacother. 127:110224.